

# A self-healing nanocomposite double network bacterial nanocellulose/gelatin hydrogel for three dimensional printing

Pejman Heidarian , Abbas Z. Kouzani \*

School of Engineering, Deakin University, Geelong, Victoria 3216, Australia



## ARTICLE INFO

**Keywords:**

Polymer-matrix composites (PMCs)  
Strength  
Mechanical properties  
Microstructures

## ABSTRACT

Extrusion-based three-dimensional (3D) printing of gelatin is important for additive manufactured tissue engineering scaffolds, but gelatin's thermal instability has remained an ongoing challenge. The gelatin tends to suddenly collapse at mild temperatures, which is a significant limitation for using it at physiological temperature of 37 °C. Hence, fabrication of a thermo-processable gelatin hydrogel adapted for extrusion-based additive manufacturing is still a challenge. To achieve this, a self-healing nanocomposite double-network (ncDN) gelatin hydrogel was fabricated with high thermo-processability, shear-thinning, mechanical strength, self-healing, self-recovery, and biocompatibility. To do this, amino group-rich gelatin was first created by combining gelatin with carboxyl methyl chitosan. Afterwards, a self-healing ncDN gelatin hydrogel was formed via an in-situ formation of imine bonds between the blend of gelatin/carboxyl methyl chitosan (Gel/CMCh) and dialdehyde-functionalized bacterial nanocellulose (dBNC). dBNC plays as nanofiber cross-linkers capable of simultaneously crosslinking and reinforcing the double networks of Gel/CMCh through formation of dynamic 3D imine bonds. Based on our findings, our self-healing ncDA gelatin hydrogel displayed great potential as a promising ink for additive manufactured tissue engineering scaffolds.

## 1. Introduction

Extrusion-based three-dimensional (3D) printing has been increasingly used as a popular additive manufacturing method to fabricate predefined structures with precise geometry and high resolution (Heidarian, Kouzani, Kaynak, Paulino, & Nasri-Nasrabadi, 2019; Kalkal et al., 2021; Placone & Engler, 2018; Wulle et al., 2022; Zhang et al., 2019; Zhou, Fu, & He, 2020). Although in this additive manufacturing technique, nozzle diameter, printing speed, and applied pressure all influence the spatial resolution of the printed object, the intrinsic properties of the materials used as inks are of great importance as well, and play a crucial role in 3D printing as they provide desired properties for the obtained objects (Ngo, Kashani, Imbalzano, Nguyen, & Hui, 2018). As a result, advancement in extrusion-based 3D printing is dependent on the design of 3D printable materials used as inks (Heidarian et al., 2019; Tytgat et al., 2019). As an example, 3D printed scaffolds can be customized to a favorable composition and morphology to create a desired biological environment in which tissue can form and grow (Nagaraj, Etxeberria, Naffa, Zidan, & Seyfoddin, 2022; Wang, Chen, Zheng, Liu, & Zhang, 2022; Zhou et al., 2020). Among different

inks used thus far for extrusion-based additive manufacturing, hydrogels stand out as one of the most promising materials for this purpose (Heidarian et al., 2019; Jacob, Passamai, Katz, Castro, & Alvarez, 2022; Krishna & Sankar, 2023; Li, Wu, Chu, & Gelinsky, 2020; Unagolla & Jayasuriya, 2020).

Hydrogels are 3D networks of hydrophilic polymers that are chemically or physically cross-linked. On a macroscopic scale, they act like solids, yet their 3D networks can hold significant volumes of water or biological fluids. Because of their similarity to native extracellular matrices (ECM), they may be used in a variety of biological applications, including tissue engineering and drug delivery systems (Zhang & Khademhosseini, 2017). Hydrogels may be utilised as inks in extrusion-based additive manufacturing provided they demonstrate strong printability and structural integrity after printing, in addition to their biocompatibility to enable cell survival and hence tissue development (Wang et al., 2022). There are different hydrophilic polymers, such as alginate (Varaprasad, Karthikeyan, Yallapu, & Sadiku, 2022), chitosan (Lazaridou, Bikaris, & Lamprou, 2022), starch (Cui et al., 2022),  $\kappa$ -carrageenan (Kumari, Mondal, & Chatterjee, 2022), etc., that can be employed for fabrication of hydrogels, among which gelatin, derived

\* Corresponding author.

E-mail address: [kouzani@deakin.edu.au](mailto:kouzani@deakin.edu.au) (A.Z. Kouzani).

from animal collagen, can be considered as one of the most extensively studied polymers in this area because it autonomously gels at room temperature without needing external additive or modification (Jaipan, Nguyen, & Narayan, 2017). It is also a non-toxic, biocompatible, water-soluble, cost-effective, and drug administration (FDA)-approved biopolymer able to be degraded enzymatically. Moreover, gelatin can prevent cell apoptosis and promote cell proliferation and differentiation, thereby accelerating tissue regeneration (Leu Alexa et al., 2021). Hence, it seems ideal to be employed for extrusion-based additive manufacturing.

On the flip side, however, gelatin shows thermal instability. The physical 3D network of gelatin hydrogel at temperatures over 30–35 °C suddenly collapses due to the cleavage of triple helices and hydrogen bonds, which is under the physiological temperatures, 37 °C (Heidarian et al., 2020a). Not only does it enormously limit the application of gelatin for many biomedical applications at physiological temperatures, but also hampers gelatin from tolerating temperature in polymer processing techniques, including extrusion-based 3D printing because it cannot be heated for controlling the viscosity of gelatin during 3D printing. Accordingly, it lacks mechanical strength and shape stability and shows low elasticity (Leu Alexa et al., 2021; Xing et al., 2014). These downsides, albeit, might be deemed as major drawbacks that limit the use of gelatin as 3D printable biopolymer inks, there are new methods that are being developed to address these challenges. The most used method for modification of gelatin applies methacryloyl groups to gelatin, aka photo-crosslinkable gelatin (Bupphathong et al., 2022; Irmak, Demirtas, Gümüşderelioglu, & Engineering, 2018; Rajabi et al., 2021; Unagolla & Jayasuriya, 2020). While these photo-crosslinkable groups can be replaced with the unstable physical 3D structure of gelatin, they form permanent, irreversible, and static bonds after formation that may either obstruct the processability of gelatin or block the printing nozzle. Moreover, due to the permanent nature of carbon–carbon covalent bonds (C=C) caused by photo-crosslinkable methacryloyl groups, they do not have self-healing ability and cannot be recovered after breaking (Wang et al., 2022).

Reversible, temporary, and dynamic crosslinks like ionic interactions, some covalent bonds, supramolecular interactions, and hydrogen bonds impart self-healing, self-recovery, and more importantly shear-thinning to hydrogels. They may undergo sol-gel transitions during printing and rebuild their 3D network after printing through shear-thinning behavior (Heidarian et al., 2019; Heidarian et al., 2020c; Wang et al., 2022; Zhu, Zhang, Wei, Zhang, & Weng, 2023). In this paper, inspired by the intrinsic ability of nature-made systems to self-heal, we use only pristine gelatin whose 3D network is constructed using temporary, reversible, dynamic imine covalent bonds that are not only thermally and mechanically stable, but also can be 3D-printed using thermo-processable extrusion-based techniques with excellent shear thinning properties. Moreover, because of the presence of temporary, reversible, dynamic imine bonds, pristine gelatin shows excellent self-healing (the ability to gain the original shape at the molecular level after damage) and self-recovery properties (the ability to repair internal damage caused by rheological deformations) (Heidarian et al., 2019; Taylor & in het Panhuis, 2016). Hence, it can be reprocessed and extruded over and over and if damaged, it can autonomously self-heal the damaged area. To achieve this, gelatin was first blended with carboxyl methyl chitosan to increase its amino groups' content. The 3D structure of gelatin hydrogel was then formed by an in-situ formation of dynamic imine bonds from the double network of gelatin/carboxyl methyl chitosan (Gel/CMCh) in the presence of dialdehyde-functionalized bacterial nanocellulose (dBNC), playing as a nanofiber cross-linker that can construct a 3D network in the blend of Gel/CMCh through the formation of imine bonds. Nanocellulose is a renewable, hydrophilic, biodegradable, and biocompatible nanomaterial, with high mechanical strength and tailorabile surface, and is currently gaining attention to resolve the present issues of dynamic hydrogels: fabrication of a robust, yet autonomous self-healing hydrogel (Chen et al., 2023;

Heidarian et al., 2021). Applying nanocellulose in a 3D network of hydrogels can lead hydrogels to meet the requirements of 3D printability as they not only can reinforce the 3D network hydrogel, but also can control the viscosity of hydrogels during 3D printing.

Herein, we employed dBNC as a dialdehyde-filled nano-reinforcement to crosslink and reinforce Gel/CMCh amino-filled matrix via the formation of imine bonds. The hydrogel was revealed to be shear-thinning, self-recoverable, and self-healable. We also evaluated the printability, as well as mechanical and structural properties of the prepared nanocomposite double-network (ncDN) gelatin hydrogel. Finally, the ncDN gelatine hydrogel's biocompatibility was tested to see whether or not it would be useful as a tissue engineering scaffold ink. The thermo-mechanical properties, 3D printability, and biocompatibility of our hydrogel suggest that it may be useful as an additive produced scaffold for tissue engineering, and to the best of the authors' knowledge, this self-healing ncDN gelatin hydrogel has not been employed yet as ink for 3D printing.

## 2. Materials and methods

Nano Novin Polymer Co. graciously supplied bacterial nanocellulose (BNC) (Iran). Sigma-Aldrich, Inc. supplied the following chemicals: sodium periodate (CAS: 7790-28-5), chitosan (CAS: 9012-76-4, medium molecular weight, 190,000–310,000 Da, deacetylation degree 75 %), and gelatin (Gel, from porcine skin, CAS: 9000-70-8).

### 2.1. Preparation of carboxymethyl chitosan (CMCh)

Carboxymethyl chitosan (CMCh) was prepared using the method reported by Bidgoli et al., with minor changes (Bidgoli, Zamani, & Taherzadeh, 2010). To alkali chitosan at room temperature, a required amount of sodium hydroxide was dissolved in 100 ml of water and combined with 50 g of chitosan and adequate amount of 2-propanol solution. The chitosan was then acetylated by adding 75 g of monochloroacetic acid to 100 ml of isopropanol drop by drop, followed by 4 h stirring at room temperature. Following this, the mixture was refluxed in a water bath at 60 °C for a further 2 h while being continuously stirred, after which the leftover solvent was discarded. After gradually adding an adequate amount of 70 % ethanol to the mixture, the chitosan acetylation reaction was terminated, and the resultant crude CMCh was dried at room temperature. After drying the crude CMCh, we diluted it with distilled water, neutralised it with an aqueous solution of hydrochloric acid, and centrifuged it to eliminate impurities (5000 g, 10 min). The last step included exposing the CMCh supernatant to distilled water at room temperature for five days. The DS was determined to be 0.89 using the Bidgoli et al. technique on freeze-dried CMCh powders kept in plastic bags until usage (Bidgoli et al., 2010).

### 2.2. Synthesis of dialdehyde-functionalized bacterial nanocellulose (dBNC)

The dialdehyde-functionalized bacterial nanocellulose (dBNC) was synthesized using the same process as Jin et al., with minor changes (Jin, Li, Xu, & Sun, 2015). Deionized water was first used to dilute bacterial nanocellulose (BNC) to 0.3 wt%. After diluting BNC, an adequate amount of sodium periodate was added while the mixture was being stirred at 40 °C for 48 h. Following the addition of an adequate amount of ethylene glycol to the dBNC suspension, the oxidation was ceased. The mixture was finally stirred for 1 h before being dialyzed with a membrane against deionized water for 72 h (MWCO 3000).

The resulting dBNC suspension was stored at 4 °C until required. The dialdehyde content of dBNC was then calculated using the Eq. (1) and estimation of imine reaction between hydroxylamine hydrochloride and the dialdehyde groups of dBNC:

$$DC \text{ (mmol g}^{-1}) = \frac{C(V_2 - V_1)}{m} \quad (1)$$

where V1 and V2 are volumes (in ml) of sodium hydroxide and hydrochloric acid, respectively, used in the dBNC titration and control titration, respectively. C is the sodium hydroxide concentration in mol l<sup>-1</sup>, and m is the sample mass in g (Jin et al., 2015).

### 2.3. Fabrication of self-healing ncDN gelatin hydrogel

The PBS solutions of CMCh (2 wt%) and Gel (2 wt%) were first mixed under stirring at different Gel to CMCh ratios: 4:1, 3:1, 2:1, and 1:1, as the NH<sub>2</sub> matrix. The Gel/CMCh at 4:1 ratio, for example, refers to a blend of Gel/CMCh containing 4 portions of gelatin and one portion of CMCh, and so forth. Based on our prior research on the distribution of nano-polysaccharides in gelatin and CMCh, we then combined different ratios of Gel/CMCh mixtures with dBNC at 1 wt% concentrations (Heidarian et al., 2022; Heidarian, Kouzani, Kaynak, Paulino, et al., 2020a). All blends at different ratios were then continuously mixed and loaded into glass vials for gelation, and gelation was confirmed with a standard inversion test. After that, each blend was prepared using a different ratio, and it was continually mixed before being poured into glass vials for the gelation process and verified using a standard inversion test.

### 2.4. Characterization of self-healing ncDN gelatin hydrogel

Fourier-transform infrared (FTIR) spectroscopy (Bruker Vertex 70 FTIR) was used for examining the spectra related to BNC, dBNC, and self-healing ncDN gelatin hydrogel. The samples were dried and powdered before being pressed into discs with KBr and scanned between 600 cm<sup>-1</sup> and 4000 cm<sup>-1</sup>. The morphologies of BNC, dBNC and the cross-section of freeze-dried self-healing ncDN gelatin hydrogel were studied using scanning electron microscopy (SEM, Zeiss). Nanofiber sizes were determined using ImageJ. The inverted-vial approach revealed that self-healing ncDN gelatin hydrogels were thermally stable. To determine the thermal stability of the 3D networks, several self-healing ncDN gelatine hydrogels were put in a 10 ml vial and inverted at 60 °C. Each self-healing ncDN gelatin hydrogel was then freeze-dried and submerged in PBS solution at 37 °C. Every 2 h, the hydrogels were weighted to determine the swelling ratios of the hydrogels. Before weighting, the hydrogels were gently wiped using an absorbent paper to remove extra water. The calculation continued until equilibrium, and measurements were determined using:

$$\text{Swelling ratio} = \frac{W_1 - W_0}{W_0} \% 100 \quad (2)$$

where dried weight (W<sub>0</sub>) and swelled weight (W<sub>1</sub>) are the respective sample weights before and after expansion. Experiments on water retention ratio were also conducted by drying the swollen hydrogel in an oven at 80 °C at different times:

$$\text{Water retention ratio} = \frac{W_t - W_d}{W_d \times \text{Swelling Ratio}} \% 100 \quad (3)$$

where W<sub>t</sub> is the weight of hydrogel after swelling at time t and W<sub>d</sub> is the weight of hydrogel after drying. The gel fraction and degradation of hydrogels were calculated by drying the hydrogels in a vacuum oven for 48 h at 60 °C to obtain the initial dried weight (W<sub>0</sub>) followed by incubating them in PBS at room temperature. Afterward, they were taken out at 2, 4, 6, 8, and 10 days, then vacuum dried for 24 h and weighed again to obtain W<sub>t</sub>. In order to compare the degradation profiles of hydrogels among formulations, we calculated the gel fraction using:

$$\text{Gel fraction} = \frac{W_t}{W_0} \% 100 \quad (4)$$

To evaluate the injectability of self-healing ncDN gelatin hydrogel, a syringe equipped with a needle was filled with the self-healing ncDN, and it was gently dispensed to draw a cube structure at different layers on a plate. The self-healing ncDN gelatin hydrogel was then placed into a disposable syringe and gently squeezed to eliminate the air before 3D printing. A 0.6 mm syringe nozzle tip was then attached to the 3D-Bioplotter machine in order to print filaments that are both continuous and stable, we adjusted the print head's speed, temperature, and pressure to 50.0 mm.s<sup>-1</sup>, 50 °C, and 1.8 bar, respectively. A rheometer with a parallel plate geometry of 40 mm in diameter and a gap of 49 μm was used to measure the rheological properties of the hydrogel (TA Instruments, HR-3). To do so, loss (G') and storage (G) moduli of the hydrogel was monitored at 1 Hz by straining the gels from 1 to 1000 %. The self-recovery ability was studied by subjecting the hydrogel to strains of 1 and 400 % strains under a continuous step strain rheology test at fixed 200 s intervals at a frequency of 1 Hz. Using the same rheometer, the viscosity of the hydrogel was determined as a function of shear rate at 50 °C. The temperature sweep of hydrogel was measured at σ = 20 Pa and frequency f = 1 Hz over the range 20 to 70 °C.

Self-healing properties of the hydrogels were shown in a macroscopic experiment by cutting hydrogels in half and connecting the halves together from the cutline without external stimuli or pressure at room temperature. Hydrogels were shown to heal by being lifted and stretched in a direction perpendicular to the cutline. Hydrogel self-repair was also seen on a microscopic scale with the use of an optical microscope (Olympus GX41 Inverted Microscope). To compare the strength of the original hydrogels (S<sub>0</sub>) and the repaired hydrogels (S<sub>h</sub>), a compression test was used to bend the hydrogels from the cutline till rupture. The self-healing efficiency (SE) of the hydrogel was measured by calculating the ratio of the repaired hydrogel's strength to the original hydrogel's strength (S<sub>h</sub>/S<sub>0</sub>). Chondrocyte cells were isolated from white New Zealand rabbit articular cartilage using a technique similar to that described by Bonakdar et al. (Bonakdar et al., 2010). Cells were grown in Dulbecco's Modified Eagles Medium (DMEM) containing 100 U/ml penicillin/streptomycin and 10 % fetal bovine serum (FBS) and kept at 37 °C in a CO<sub>2</sub> incubator. Then, the cells were seeded on the various ncDN gelatine hydrogels and cultured at 37 °C in a humidified 5 % CO<sub>2</sub> atmosphere. The MTT assay was used to measure the proliferation of each sample on days 1–3. 100 μl of 3-(4, 5-dimethylthiazol-2-yl)-2, 5-diphenyltetrazolium-bromide solution was added to each sample, and they were incubated for 4 h. A 100 μl of dimethyl sulfoxide (DMSO) was used to dissolve purple formazan crystals. The absorbance of each sample was determined at 545 nm using a multi well microplate reader. After 3 days in culture, cells were stained with ethidium homodimer (red, showing the dead cells) and calcein-AM (green, showing the living cells) and images were taken using a confocal laser scanning microscope to evaluate cell adherence to the 3D printed scaffolds (LSM710, Carl Zeiss, Germany).

## 3. Results and discussion

### 3.1. Synthesis, gelation, swelling behavior, and thermo-stability

When gelatin concentrations rise over 2 wt%, the polymer chains in the gelatin undergo a conformational shift, going from random coils to triple helices maintained by intermolecular hydrogen bonds. This results in gelation of gelatin. However, the physical gelation of gelatin is not thermally stable and tends to collapse over 30–35 °C (Fig. 1a). This limits the usage of gelatin, especially under physiological conditions (Heidarian, Kouzani, Kaynak, Paulino, et al., 2020a; Xing et al., 2014). Here, it is expected that by introducing imine bonds, the weak, thermo-sensitive 3D network of gelatin can significantly be improved. The condensation reaction between dialdehyde groups and amine compounds results in a reversible, dynamic covalent bond known as the imine reaction (-N=CH-), and is a feasible technique for creating autonomous self-healing hydrogels with good printability and

biocompatibility under neutral conditions (Heidarian et al., 2022). The dialdehyde groups can be introduced to polymers using periodate-oxidation that breaks the C-2/C-3 hydroxyl groups in the glucose unit of polymer chains and convert them into dialdehyde groups (Wang, Xiao, Peng, Chen, & Fu, 2019). So far, many oxidized biopolymers have been synthesized using this method; however, oxidation dramatically reduces the molecular weight of the polymer used as a matrix (Yeo & Park, 2021). To avoid this, the self-healing ncDN gelatin hydrogels were fabricated *in situ* by a blend of Gel/CMCh as the amino-filled double network matrix, and dialdehyde groups were introduced to pristine hydroxyl groups of BNC using periodate-oxidation to form dBNCs as the dialdehyde-filled nanofiber cross-linker. By doing so, the matrix will remain intact from oxidation. Fig. 1b shows the results of FTIR analysis of BCNs and dBNCs, which showed a new peak at  $1732\text{ cm}^{-1}$  in the dBNCs spectra, showing the successful incorporation of dialdehyde groups on dBNCs (Jin et al., 2015; Xu et al., 2019). Another indicator that the C2 and C3 hydroxyl groups converted to dialdehyde groups is provided by the dialdehyde content of dBNCs, which was calculated to be  $8.14\text{ mmol g}^{-1}$  using Eq. (1) according to the technique developed by Jin et al. (Jin et al., 2015). Fig. 1c and d illustrate the morphology of BNC and dBNC. According to the frequency data (Fig. 1e), the majority of both BNC and dBNC had a diameter of 40–50 nm, demonstrating that oxidation has no effect on the overall morphology of the nanofibers, and dBNC can impart a good nano-reinforcing effect to the hydrogel. Imine reactions on the gelation and thermo-stability of self-healing ncDN gelatine hydrogels were evaluated using a vial inversion test (Video S1, Supplementary information) and FTIR analyses (Fig. 1b).

It was observed that by including dBNC to Gel/CMCh blend at a 4:1 ratio the hydrogel was not able to endure  $60\text{ }^\circ\text{C}$  because its 3D network collapsed and the hydrogel flowed. However, by increasing the portion of CMCh content in the Gel/CMCh blend, the 3D network was reinforced to endure  $60\text{ }^\circ\text{C}$ . At the 3:1 and 2:1 Gel/CMCh ratios, the double network of gelatin went to a semi-solution and semi-gel state after 20 min, while the hydrogel fabricated with an equal ratio of Gel/CMCh (1:1) was able to withstand the hot bath water without losing its 3D structure (Fig. 1f). Thus, this observation shows that by increasing CMCh, the content of imine reactions between CHO and NH<sub>2</sub> increases, which leads to higher crosslinking density and more thermally stable 3D networks (Li et al., 2020; Liu et al., 2018; Wei et al., 2015). This finding also demonstrates the inability of gelatin to create imine bonds at a high ratio of Gel to CMCh, 4:1, because of its low concentration of amino groups. FTIR spectra were also used to track the development of imine linkages in the self-healing ncDN gelatin hydrogels (Fig. 1b). The imine ncDN gelatin hydrogel was formed when the -NH<sub>2</sub> groups of Gel/CMCh and the -CHO groups of dBNC reacted, and the resulting reaction exhibited two peaks at  $1599\text{ cm}^{-1}$  and  $1695\text{ cm}^{-1}$  corresponding to the C=N double bond stretching vibration. Furthermore, the distinctive peak of -CNO in dBNC, at  $1732\text{ cm}^{-1}$ , was missing from the spectra of the self-healing ncDN gelatine hydrogels, likely as a result of imine synthesis and dialdehyde consumption.

Many aspects of the hydrogel, including oxygen transfer and nutrition penetration, are influenced by the swelling ratio. Simultaneously, numerous elements influence the hydrogel's swelling ratio, including the polymer's concentration and hydrophilicity, composition, and network structure (Wang et al., 2022). Hydrogel swelling was measured after being incubated in PBS solution at  $37\text{ }^\circ\text{C}$  for different times. As shown in Fig. 1g, there is a considerable rise in swelling rate from the first 2 h, but after that, the samples gradually reached equilibrium in 12 h. Furthermore, the swelling ratio of the hydrogel was shown to be influenced by the hydrogel CMCh's content. Raising the content of CMCh from the matrix with the Gel/CMCh of 4:1 to a matrix with the Gel/CMCh of 1:1 decreased the swelling ratio of the hydrogels from 543.3 to 227.7 g<sub>water</sub>/g<sub>absorbent</sub>. The lower swelling ratio might be because as the content of CMCh increases, the polymer chains were more densely entangled, resulting in a denser imine cross-linked network. This slower swelling is a direct effect of the decreased pore size, which restricts the

passage of water molecules. We then measured the water retention ability of hydrogels by first swelling them in distilled water to equilibrium and then heating them at  $80\text{ }^\circ\text{C}$  at different time intervals. As demonstrated in Fig. S1, the hydrogels' capacity to retain water improved with increasing CMCh ratio probably due to the increased crosslinking density. Gel fraction and degradation rates of hydrogels with different Gel/CMCh ratios were measured using the procedure presented by Nagaraj et al. (Nagaraj et al., 2022). As demonstrated in Fig. S2, the gel fraction of hydrogels was reduced by increasing CMCh in the matrix, and the Gel/CMCh hydrogel with 1:1 ratio showed the lowest degradability, which can be related to the improved cross-linking density. By day 10, almost all of the samples were degraded and the gel fraction for hydrogels containing 4:1, 3:1, 2:1, and 1:1 were found to be at 1.23, 3.69, 6.40, and 8.86 %. Fig. 1j shows the scheme of imine bonds in the hydrogel.

### 3.2. Self-healing and morphology

The self-healing capacity of imine linkages was assessed by cutting disc-shaped hydrogels in half at all Gel/CMCh ratios and then contacting them along the cutline at both ambient and physiological temperatures without utilizing force, external stimuli, or additive. Half of the disc-shaped hydrogels were coloured with rhodamine B dye to highlight the self-healing process. After 12 h, the hydrogels at varied Gel/CMCh ratios self-healed completely and could be lifted under gravity from the cutline in a full disc form structure, as illustrated in Fig. 2(a-d). At room temperature, the optical microscope photos were collected to demonstrate the healing process at the interface of self-healing ncDN gelatine hydrogel with a 3:1 Gel/CMCh ratio (Fig. 2e-j). As shown, the gap at the interface of the sliced hydrogel was very large at the start of the healing process, but it decreased dramatically over the healing process, to the point that the sign of the crack was scarcely discernible at the repaired hydrogel's junction after 24 h. SEM pictures of freeze-dried hydrogels at 3:1 (Fig. 2k), 2:1 (Fig. 2l), and 1:1 (Fig. 2m) Gel/CMCh ratios after 24 h of self-healing are shown in Fig. 2. These hydrogels exhibit excellent self-healing properties, since there is no obvious difference between the uncut and repaired areas and the boundaries are not distinguishable. Due to the high miscibility between gelatin and CMCh polymer chains, the self-healing freeze-dried hydrogels produced have a highly interconnected porous structure and semi-interpenetrated network, with nearly identical, homogeneous, interconnected pore sizes that are conducive to cell viability and nutrition exchange.

As shown in the SEM images, the pore sizes slightly decreased by increasing CMCh content presumably because of the formation of a more interpenetrated network in the matrix that can boost the internal crosslinking density of imine bonds (Li, Wang, et al., 2020; Wang et al., 2022). These observations also reveal the good autonomous self-healing and microstructure regeneration ability of this self-healing ncDN gelatin hydrogel outperforming previous research (Asoh, Kawai, & Kikuchi, 2014; Hu, Cheng, & Zhang, 2015). It also reveals that imine bonds, rather than being a simple adhesion between the damaged areas, generate strong intermolecular bridges between the cutline of fractured hydrogels (Li, Wang, et al., 2020; Wei et al., 2015). Video S2, Supplementary Information, shows the capability of self-healed ncDN gelatin hydrogels at a 3:1 Gel/CMCh ratio to tolerate strain and stress after 24 h healing. At room temperature and  $37\text{ }^\circ\text{C}$ , we performed a compression test to determine the hydrogels' SE (after 24 h of self-healing), where SE is defined as the ratio of self-healed strength ( $S_h$ ) over the original strength ( $S_o$ ), as shown in Fig. 2(n-p). As shown in Fig. 2p, the SE of hydrogels was found to be 60 % in the hydrogels with a Gel/CMCh ratio of 4:1 presumably due to the low formation of imine bonds, low viscosity of the hydrogel, and insufficient content of amino groups in gelatin (Lei et al., 2019). Although the SE reached the highest value at Gel/CMCh ratio of 3:1 (84 %), a further increase of CMCh resulted in a steady drop in SE with 75 % SE at 1:1 Gel/CMCh ratio, which might be attributed to the increased viscosities and highly cross-linked regions in the hydrogel

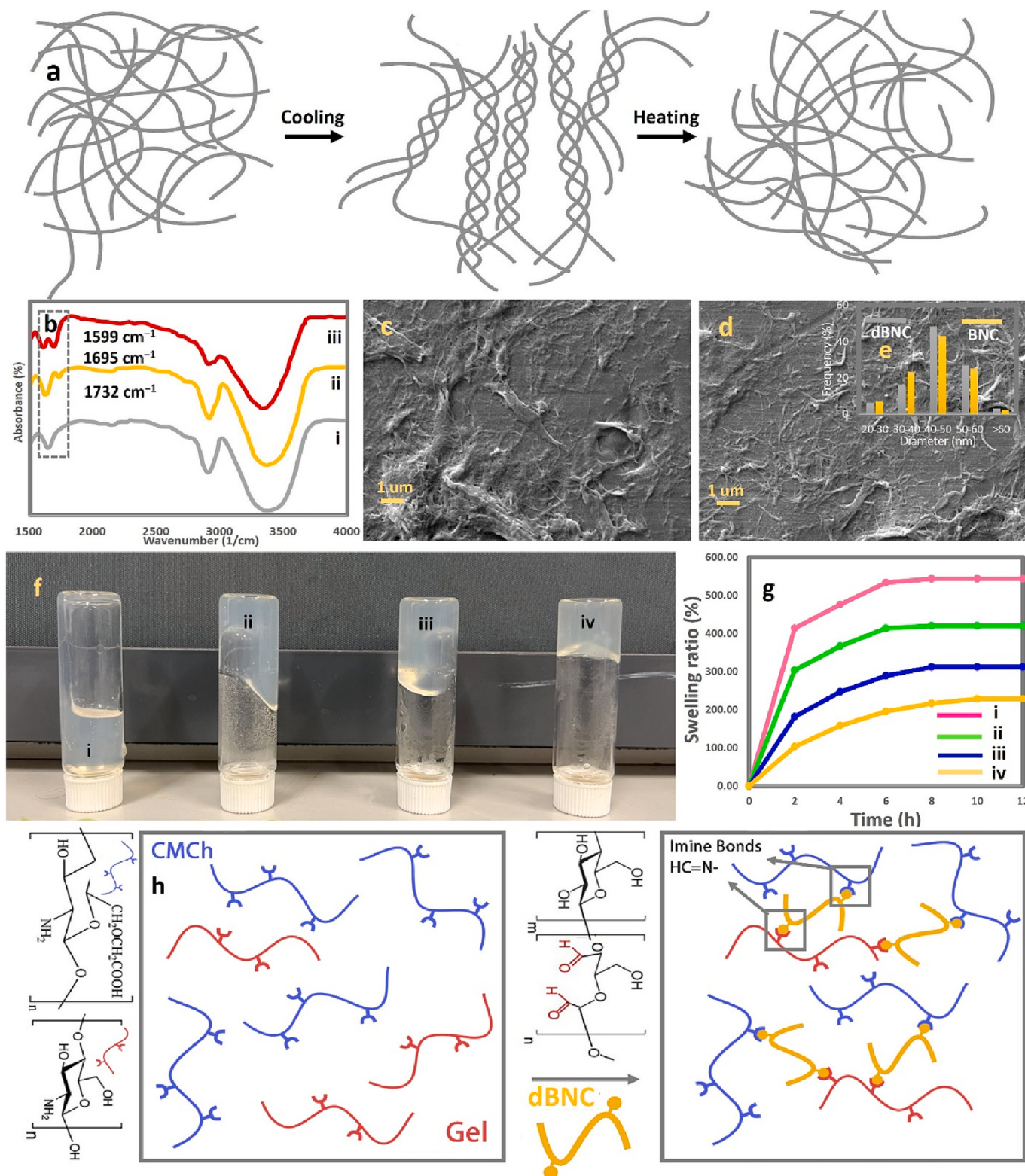


**Fig. 1.** (a) Gelatin physical gelation due to conformational change in polymer chains from random coils to triple helices and destruction of physical bonds by applying temperature (b) FTIR spectra of (i) BNC, (ii) dBNC, (iii) self-healing ncDN gelatin hydrogel at Gel/CMCh = 4:1, SEM images of (c) BNC, (d) dBNC, (e) frequency of nanofibers at different diameters, (f) thermo-stability of self-healing ncDN gelatin hydrogel at different Gel/CMCh ratios (i) 4:1, (ii) 3:1, (iii) 2:1, (iv) 1:1, (g) swelling ratio of self-healing ncDN gelatin hydrogel at different Gel/CMCh ratios (i) 4:1, (ii) 3:1, (iii) 2:1, (iv) 1:1, and (j) schematic representation of the ncDN hydrogel's self-healing properties.

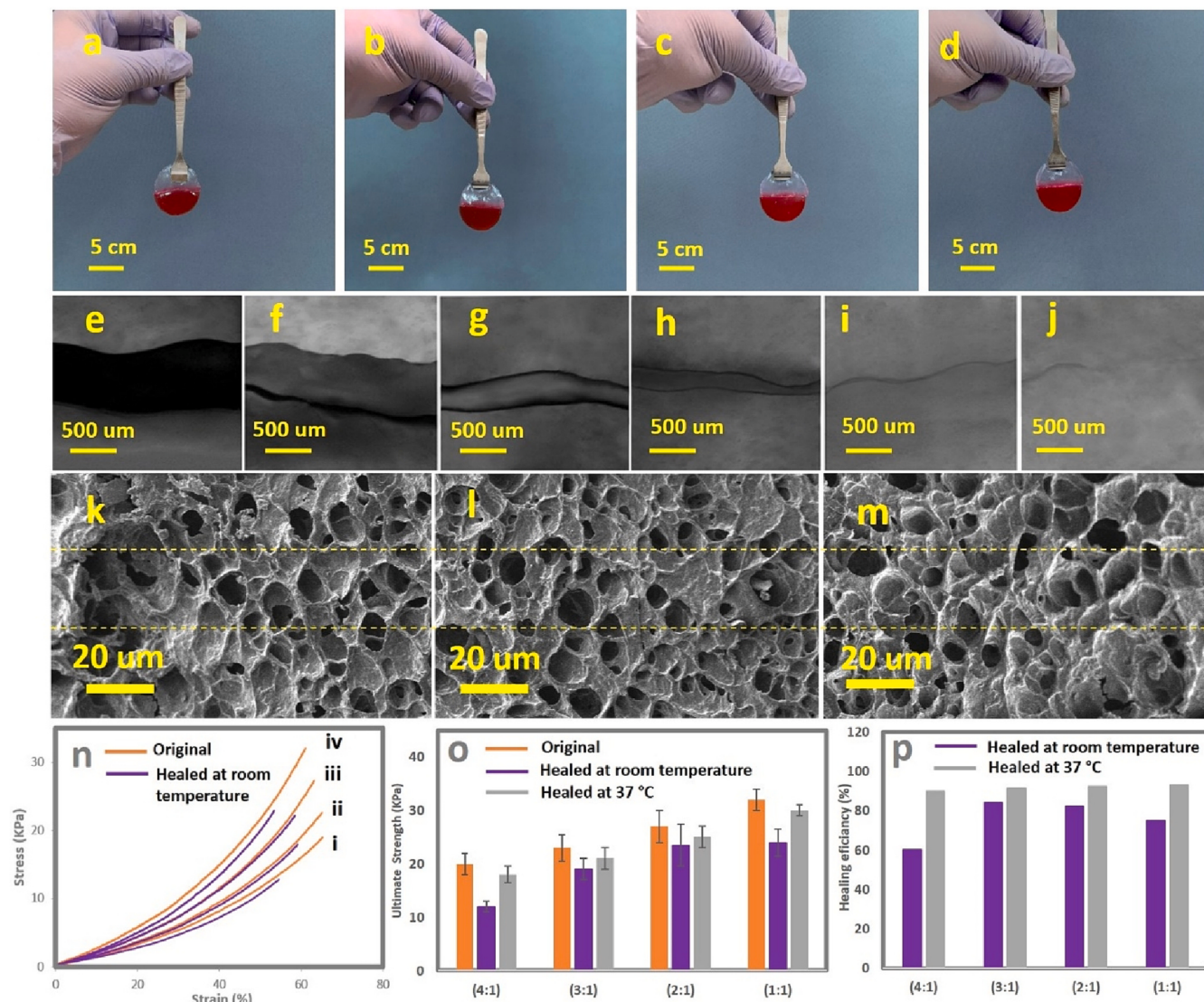


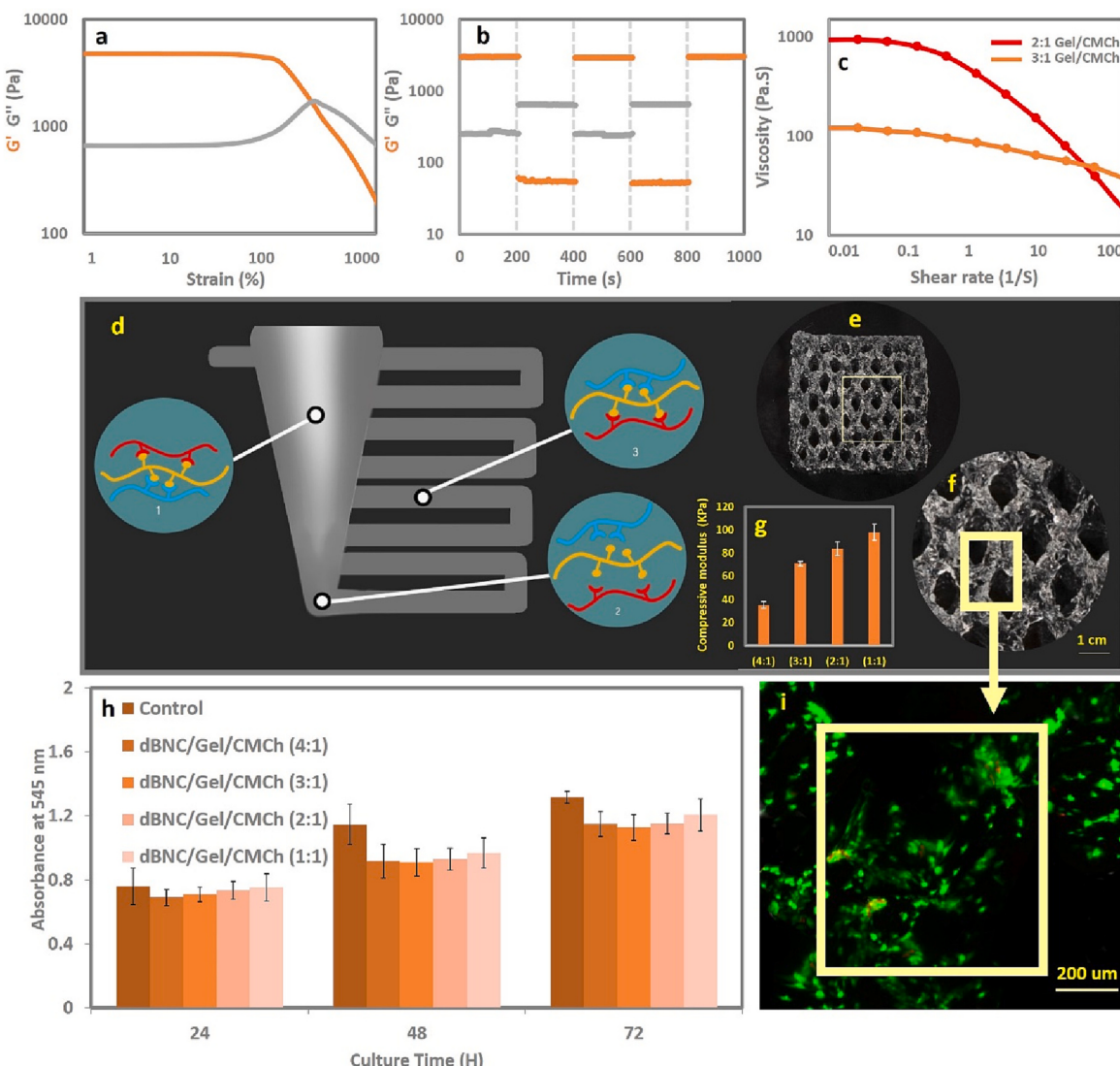
**Fig. 2.** Lifting self-healed ncDN gelatin hydrogels from the cutline at different ratios after 12 h self-healing (a) Gel/CMCh (4:1), (b) Gel/CMCh (3:1), (c) Gel/CMCh (2:1), (d) Gel/CMCh (1:1), optical microscopy images of the hydrogel with the Gel/CMCh of 3:1 at room temperature and different healing time (e) just cut hydrogel, (f) after 3 h healing, (g) after 6 h healing, (h) after 9 h healing, (i) after 12 h healing, (j) after 24 h healing, the SEM images of self-healed freeze-dried ncDN gelatin hydrogel at (k) 3:1 Gel/CMCh, (l) 2:1 Gel/CMCh, (m) 1:1 Gel/CMCh after 24 h healing, (n) typical stress–strain curves of the healed and original hydrogels at different ratios after 24 h self-healing, (i) Gel/CMCh (4:1), (ii) Gel/CMCh (3:1), (iii) Gel/CMCh (2:1), (iv) Gel/CMCh (1:1), (o) hydrogels' maximum strength at 37 °C and room temperature, (p) hydrogels' ability to self-heal at ambient temperature and 37 °C.

that may pose an impact on the molecular mobility of polymer chains, thus self-healing performance (Wei et al., 2015). Hence, the ncDN gelatin with a 3:1 ratio provided the highest SE at room temperature. Because higher temperatures may increase the dynamic kinetics and molecular mobility of reversible bonds, the SE of all self-healing ncDN gelatin hydrogels significantly achieved above 90 % when compared to their counterparts at ambient temperature (Fig. 2p), which is an evidence that the hydrogel may have better self-healing performance under physiological conditions than room temperature (Wei et al., 2015).

### 3.3. 3D printability and biocompatibility

3D printing can advance the fabrication of better engineered scaffolds for tissue engineering, but this advancement depends on developing printable biomaterials, such as hydrogels. In order for hydrogels to be printable, they must show shear-thinning behavior during a 3D printing process, and rapid self-recovery from a sole state to a gel state after printing. Moreover, their viscosity not only must be in a printable

range to facilitate extrusion, but also it must increase immediately after printing to form stable filaments while showing enough mechanical strength and integrity to maintain the printed structures (Heidarian et al., 2019; Leu Alexa et al., 2021; Spicer, 2020). Hydrogels need to create homogenous and stable filaments during the extrusion and solidify promptly after printing in order to fulfil the extrusion-based 3D printability criteria. They are needed for the gel's structural integrity and to provide it enough mechanical strength to last (Heidarian et al., 2019). Herein, we fabricated an ncDN gelatin hydrogel containing imine bonds with improved mechanical strength and self-healing capabilities that might be used as an ink in extrusion-based additive manufacturing. For this purpose, we first examined the shear-thinning, self-recovery, and viscosity of the hydrogel as three important requirements for the injectability and printability of a hydrogel (Alarçin et al., 2018). At Gel/CMCh 3:1 ratio and ambient temperature, the shear-thinning behavior and gel–sol transition point of the hydrogel were investigated using strain amplitude scanning. Fig. 3a shows the result of the amplitude scanning. As seen, the rheological measurement indicated the formation



of stable elastic 3D bonds because the loss modulus ( $G''$ ) was positioned lower than the storage modulus ( $G'$ ). However, when strain was increased,  $G'$  dropped dramatically, revealing the hydrogel's strong shear-thinning tendency and flowability. The findings showed that at 345 %, the hydrogel transitioned from a solid to a liquid and  $G''$  became greater than the  $G'$  owing to shear-thinning behavior, as seen in Fig. 3a. (Heidarian et al., 2020b). This also means the collapse of imine bonds (sol-state) at strains higher than 345 %. For evaluation of the self-recovery and breakup and reformation of the hydrogel network, 1 and 400 % strains were selected under a continuous step strain rheology test at fixed 200 s intervals (Fig. 3b). Based on the findings, the hydrogel network is stable for moderate stresses, since the  $G'$  was greater than the  $G''$  and did not change over time when exposed to 1 % strain. When the hydrogel was broken by a rapid change in strain to 400 %, the  $G'$  and  $G''$  converted ( $G'' > G'$ ), showing the collapse of the 3D network. Upon resetting the strain to 1 %, both  $G'$  and  $G''$  readings quickly reverted to near-initial levels, with  $G'$  being greater than  $G''$ . As depicted in Fig. 3b,

the hydrogel was disrupted again by raising the strain to 400 % causing  $G''$  to rise above  $G'$  ( $G' < G''$ ) and destruction of the 3D imine network, but  $G'$  was immediately restored to its original value after the prompt restoration of the strain to 1 %. These findings demonstrate that hydrogels can self-recover quickly and efficiently at the molecular level, which is an ideal behavior for 3D printing of the hydrogel and lends credence to the hydrogel's self-healing abilities. The observed rapid self-recovery is also the behavior that biological tissues, including tendons, cartilage, and muscles inherently possess as it assists the tissue in absorbing and dissipating a portion of the external stress (Wang et al., 2022). The thermal transition of the ncDN gelatin hydrogels at 3:1 Gel/CMCh ratio occurred at 65 °C (Fig. S3), where the hydrogel flows and  $G''$  surpasses  $G'$  with just a little rise in temperature. For injecting or printing the hydrogel, this temperature is essential. Hydrogels with the proper viscosities are required for extrusion-based additive manufacturing, so the viscosity of the ncDN gelatin hydrogels at 3:1 and 2:1 Gel/CMCh ratios were tested before printing at 50 °C. This

temperature, loses the imine bonds but does not destroy them, thus making the extrusion smoother. As seen in Fig. 3c, the viscosity increased with increasing the Gel/CMCh ratio from 3:1 to 2:1 meaning that the viscosity is adjustable with the Gel/CMCh ratio, but it decreased at each ratio by increasing the shear rate because of the destruction of imine bonds at high shears and the shear-thinning behavior of the hydrogel.

To observe the injectability and flowability of hydrogel, a syringe was filled with the hydrogel at a Gel/CMCh ratio of 3:1 and a cube structure was drawn on a plate at different layers using a 20-gauge needle without clogging (Video S3, Supplementary Information). As seen in Video S3, the hydrogel shows good shear-thinning behavior while injecting with an instant self-recovery from a sole state to a gel state after injection. Moreover, the viscosity is not only in a printable range facilitating the injection, but also it increases rapidly after injection and forms stable filaments, with enough mechanical strength and integrity to maintain the cube's structure. Finally, a fourth-generation 3D Bioplotter (EnvisionTEC GmbH, Germany) was used to test the hydrogel's printability. To accomplish so, a polythene injection cartridge was filled with the hydrogel at a 3:1 Gel/CMCh ratio, and in the Bio-plotter software, a lattice CAD model file ( $30 \times 30$  mm) was loaded. Fig. 3d shows the schematic of the 3D printing process in three main steps. At  $50^{\circ}\text{C}$ , the hydrogel was effectively extruded via a  $580 \mu\text{m}$  diameter nozzle with a pressure of 1.8 bar and a printing speed of  $50 \text{ mm s}^{-1}$  (Video S4, Supplementary Information). Because of shear thinning, the viscosity of the hydrogel dropped during extrusion, and the ink went through the printing nozzle. The shear enforced on the hydrogel was removed when it was squeezed out of the printing nozzle, and stable hydrogel filaments were printed due to the reformation of the imine bonds. Herein, imine bonds also facilitated the connections of the printed filament layers on top of each other after printing. Finally, a stable scaffold framework was created for the printed scaffold (about  $30 \text{ mm} \times 30 \text{ mm} \times 3 \text{ mm}$ ) with 9 layers (Fig. 3e-f).

Hydrogels' mechanical strength is a crucial factor in determining their usefulness as a scaffold for tissue engineering. Based on the stress-strain curve of the unaltered samples shown in Fig. 2n at room temperature, we can calculate the compression moduli of self-healing ncDN gelatin hydrogels at different ratios. As illustrated in Fig. 3g, the compression moduli of self-healing ncDN gelatin hydrogels increased from  $35 \pm 3$  to  $98 \pm 7 \text{ kPa}$  when CMCh/Gel ratio was changed from 4:1 to 1:1, indicating that amino groups of Gel/CMCh and the dialdehyde groups of dBNCs can form more imine bonds, resulting in increased hydrogel modulus of the hydrogel. The compression moduli of the self-healing ncDN gelatin hydrogels at 3:1 Gel/CMCh ratio was doubled than that of the hydrogel at 4:1 Gel/CMCh ratio and the compression moduli of 1:1 Gel/CMCh hydrogel was three times higher than that of the hydrogel at 4:1 Gel/CMCh ratio that meets the mechanical-strength needed for tissue engineering scaffolds.

Scaffolds are a biomimetic extracellular matrix used in tissue engineering to promote cell growth and proliferation. To create a 3D printed scaffold with uniform interconnections and high mechanical strength, we employed a self-healing ncDN gelatin hydrogel as the ink. In order to create a 3D-printed scaffold, gelatin, CMCh, and BNC were chemically modified to form imine linkages and then extruded. Therefore, the hydrogel's biocompatibility was evaluated to see whether or not it could be used as a 3D printed scaffold in tissue engineering. The fabricated hydrogels were found to be non-cytotoxic and had high biocompatibility, as evidenced by the MTT experiment. The vitality of chondrocyte cells on hydrogels after 24, 48, and 72 h are shown in Fig. 3h. Based on the findings, there was no statistically significant difference in cell proliferation rates between cells seeded on hydrogels and cells seeded on tissue culture plates (as a control), and cell viability values were almost equivalent to the control. Furthermore, the 3D printed scaffold allowed cells to adequately adhere to the printed structures' surfaces. After 3 days in culture, scaffolds were visualized by labelling cells with calcein-AM (Fig. 3i). This image indicates that the cell viability is high after 3

days, and no obvious dead cells are visible. Therefore, these hydrogels may be classified as human-friendly materials that can be applied to human-related applications, which is an important prerequisite for tissue engineering hydrogel.

#### 4. Conclusion

A self-healing 3D-printable nanocomposite double network (ncDN) gelatin hydrogel was fabricated in situ by blending gelatin (Gel) and carboxyl methyl chitosan (CMCh) as the amino-filled matrix and dialdehyde-functionalized bacterial nanocellulose (dBNC) as the dialdehyde-filled nanofiber crosslinker. This formulation can form biocompatible imine reactions with nano-reinforcing effects, thus improving the mechanical properties of the object. This 3D-printable gelatin-based hydrogel also revealed high thermal stability and stable filaments during extrusion-based 3D printing at temperatures above  $37^{\circ}\text{C}$  (the temperature at which pristine gelatin normally becomes a solution due to the breakage of hydrogen bonds). As a result of imine bond formation, it also displays shear-thinning and dynamic properties, such as self-healing and self-recovery in a neutral and physiological environment without the use of any external stimuli or additives, as confirmed by macroscopic and microscopic observations and rheological measurements. Cell encapsulation exhibited cytocompatibility in the hydrogel as well. Therefore, because of the observed 3D printability and biocompatibility, we feel our self-healing hydrogel is promising for application as 3D printable inks in biomedical domains.

Supplementary data to this article can be found online at <https://doi.org/10.1016/j.carbpol.2023.120879>.

#### CRediT authorship contribution statement

**Pejman Heidarian:** Conceptualization, Methodology, Validation, Formal analysis, Investigation, Data curation, Writing – original draft, Writing – review & editing, Visualization. **Abbas Z. Kouzani:** Conceptualization, Methodology, Resources, Writing – review & editing, Supervision, Project administration.

#### Declaration of competing interest

The authors declare that they have no known competing financial interests or personal relationships that could have appeared to influence the work reported in this paper.

#### Data availability

No data was used for the research described in the article.

#### Acknowledgment

Nano Novin Polymer Co. (Sari, Iran) and Dr. Hoessin Yousefi are acknowledged to kindly prepare bacterial cellulose for this study.

#### References

- Alarçın, E., Lee, T. Y., Karuthedom, S., Mohammadi, M., Brennan, M. A., Lee, D. H., & Zhang, Y. S. (2018). Injectable shear-thinning hydrogels for delivering osteogenic and angiogenic cells and growth factors. *Biomaterials Science*, 6(6), 1604–1615.
- Asoh, T.-A., Kawai, W., & Kikuchi, A. (2014). Alternating-current electrophoretic adhesion of biodegradable hydrogel utilizing intermediate polymers. *Colloids and Surfaces B: Biointerfaces*, 123, 742–746.
- Bidgoli, H., Zamani, A., & Taherzadeh, M. J. (2010). Effect of carboxymethylation conditions on the water-binding capacity of chitosan-based superabsorbents. *Carbohydrate Research*, 345(18), 2683–2689.
- Bonakdar, S., Emami, S. H., Shokrgozar, M. A., Farhadi, A., Ahmadi, S. A. H., & Amanzadeh, A. (2010). Preparation and characterization of polyvinyl alcohol hydrogels crosslinked by biodegradable polyurethane for tissue engineering of cartilage. *Materials Science Engineering C*, 30(4), 636–643.

- Bupphathong, S., Quiroz, C., Huang, W., Chung, P.-F., Tao, H.-Y., & Lin, C.-H. (2022). Gelatin methacrylate hydrogel for tissue engineering Applications—A review on material modifications. *Pharmaceutics*, 15(2), 171.
- Chen, Z., Hu, Y., Shi, G., Zhuo, H., Ali, M. A., Jamróz, E., & Peng, X. (2023). Advanced flexible materials from nanocellulose. *Advanced Functional Materials*, 2214245.
- Cui, C., Jia, Y., Sun, Q., Yu, M., Ji, N., Dai, L., & Sun, Q. (2022). Recent advances in the preparation, characterization, and food application of starch-based hydrogels. *Carbohydrate Polymers*, 119624.
- Heidarian, P., Gharaie, S., Yousefi, H., Paulino, M., Kaynak, A., Varley, R., & Kouzani, A. Z. (2022). A 3D printable dynamic nanocellulose/nanochitin self-healing hydrogel and soft strain sensor. *Carbohydrate Polymers*, 119545.
- Heidarian, P., Kaynak, A., Paulino, M., Zolfagharian, A., Varley, R. J., & Kouzani, A. Z. (2021). Dynamite nanocellulose hydrogels: Recent advancements and future outlook. *Carbohydrate Polymers*, 270, Article 118357.
- Heidarian, P., Kouzani, A. Z., Kaynak, A., Paulino, M., & Nasri-Nasrabadi, B. (2019). Dynamic hydrogels and polymers as inks for three-dimensional printing. *ACS Biomaterials Science Engineering*, 5(6), 2688–2707.
- Heidarian, P., Kouzani, A. Z., Kaynak, A., Paulino, M., Nasri-Nasrabadi, B., & Varley, R. (2020a). Double dynamic cellulose nanocomposite hydrogels with environmentally adaptive self-healing and pH-tuning properties. *Cellulose*, 27(3), 1407–1422.
- Heidarian, P., Kouzani, A. Z., Kaynak, A., Paulino, M., Nasri-Nasrabadi, B., & Varley, R. J. (2020b). Double dynamic cellulose nanocomposite hydrogels with environmentally adaptive self-healing and pH-tuning properties. *Cellulose*, 27(3), 1407–1422.
- Heidarian, P., Kouzani, A. Z., Kaynak, A., Paulino, M., Nasri-Nasrabadi, B., & Zolfagharian, A., & Varley, R. (2020). Dynamic plant-derived polysaccharide-based hydrogels. *Carbohydrate Polymers*, 231, Article 115743.
- Hu, L., Cheng, X., & Zhang, A. (2015). A facile method to prepare UV light-triggered self-healing polyphosphazenes. *Journal of Materials Science*, 50(5), 2239–2246.
- İrmak, G. L., Demirtaş, T. R. T., Gümrüşerelioğlu, M. E., & Engineering. (2018). Highly methacrylated gelatin bioink for bone tissue engineering. *ACS Biomaterials Science Engineering*, 5(2), 831–845.
- Jacob, G. T., Passamai, V. E., Katz, S., Castro, G. R., & Alvarez, V. (2022). Hydrogels for extrusion-based bioprinting: General considerations. *Bioprinting*, 27, Article e00212.
- Jaipal, P., Nguyen, A., & Narayan, R. J. (2017). Gelatin-based hydrogels for biomedical applications. *MRS Communications*, 7(3), 416–426.
- Jin, L., Li, W., Xu, Q., & Sun, Q. (2015). Amino-functionalized nanocrystalline cellulose as an adsorbent for anionic dyes. *Cellulose*, 22(4), 2443–2456.
- Kalkal, A., Kumar, S., Kumar, P., Pradhan, R., Willander, M., Packirisamy, G., & Malhotra, B. D. (2021). Recent advances in 3D printing technologies for wearable (bio) sensors. *Additive Manufacturing*, 46, Article 102088.
- Krishna, D. V., & Sankar, M. R. (2023). Extrusion based bioprinting of alginate based multicomponent hydrogels for tissue regeneration applications: State of the art. *Materials today Communications*, 105696.
- Kumari, S., Mondal, P., & Chatterjee, K. (2022). Digital light processing-based 3D bioprinting of κ-carrageenan hydrogels for engineering cell-loaded tissue scaffolds. *Carbohydrate Polymers*, 290, Article 119508.
- Lazaridou, M., Bikaris, D. N., & Lamprou, D. A. (2022). 3D bioprinted chitosan-based hydrogel scaffolds in tissue engineering and localised drug delivery. *Pharmaceutics*, 14(9), 1978.
- Lei, J., Li, X., Wang, S., Yuan, L., Ge, L., Li, D., & Mu, C. (2019). Facile fabrication of biocompatible gelatin-based self-healing hydrogels. *ACS Applied Polymer Materials*, 1 (6), 1350–1358.
- Leu Alexa, R., Iovu, H., Ghitman, J., Serafim, A., Stavarache, C., Marin, M.-M., & Ianchis, R. (2021). 3d-printed gelatin methacryloyl-based scaffolds with potential application in tissue engineering. *Polymers*, 13(5), 727.
- Li, J., Wu, C., Chu, P. K., & Gelinsky, M. (2020). 3D printing of hydrogels: Rational design strategies and emerging biomedical applications. *Materials Science Engineering: R Reports*, 140, Article 100543.
- Li, W., Wang, B., Zhang, M., Wu, Z., Wei, J., Jiang, Y., & Chen, S. (2020). All-natural injectable hydrogel with self-healing and antibacterial properties for wound dressing. *Cellulose*, 27(5), 2637–2650.
- Liu, H., Li, C., Wang, B., Sui, X., Wang, L., Yan, X., & Mao, Z. (2018). Self-healing and injectable polysaccharide hydrogels with tunable mechanical properties. *Cellulose*, 25(1), 559–571.
- Nagaraj, A., Etxeberria, A. E., Naffa, R., Zidan, G., & Seyfoddin, A. (2022). 3D-printed hybrid Collagen/GelMA hydrogels for tissue engineering applications. *Biology*, 11 (11), 1561.
- Ngo, T. D., Kashani, A., Imbalzano, G., Nguyen, K. T., & Hui, D. (2018). Additive manufacturing (3D printing): A review of materials, methods, applications and challenges. *Composites Part B: Engineering*, 143, 172–196.
- Placone, J. K., & Engler, A. J. (2018). Recent advances in extrusion-based 3D printing for biomedical applications. *Advanced Healthcare Materials*, 7(8), 1701161.
- Rajabi, N., Rezaei, A., Kharaziha, M., Bakhsheshi-Rad, H. R., Luo, H., RamaKrishna, S., & Berto, F. (2021). Recent advances on bioprinted gelatin methacrylate-based hydrogels for tissue repair. *Tissue Engineering Part A*, 27(11–12), 679–702.
- Spicer, C. D. (2020). Hydrogel scaffolds for tissue engineering: The importance of polymer choice. *Polymer Chemistry*, 11(2), 184–219.
- Taylor, D. L., & in het Panhuus, M. (2016). Self-healing hydrogels. *Advanced Materials*, 28 (41), 9060–9093.
- Tytgat, L., Van Damme, L., Declercq, H., Thienpont, H., Otteveare, H., Arevalo, M. D. P. O., & Van Vlierberghe, S. (2019). Extrusion-based 3D printing of photo-crosslinkable gelatin and κ-carrageenan hydrogel blends for adipose tissue regeneration. *International Journal of Biological Macromolecules*, 140, 929–938.
- Unagolla, J. M., & Jayasuriya, A. C. (2020). Hydrogel-based 3D bioprinting: A comprehensive review on cell-laden hydrogels, bioink formulations, and future perspectives. *Applied Materials Today*, 18, Article 100479.
- Varaprasad, K., Karthikeyan, C., Yallapu, M. M., & Sadiku, R. (2022). The significance of biomacromolecule alginate for the 3D printing of hydrogels for biomedical applications. *International Journal of Biological Macromolecules*, 212, 561–578.
- Wang, Y., Chen, Y., Zheng, J., Liu, L., & Zhang, Q. (2022). Three-dimensional printing self-healing Dynamic/Photocrosslinking gelatin-hyaluronic acid double-network hydrogel for tissue engineering. *ACS Omega*, 7(14), 12076–12088.
- Wang, Y., Xiao, G., Peng, Y., Chen, L., & Fu, S. J. C. (2019). Effects of cellulose nanofibrils on dialdehyde carboxymethyl cellulose based dual responsive self-healing hydrogel. 26(16), 8813–8827.
- Wei, Z., Yang, J. H., Liu, Z. Q., Xu, F., Zhou, J. X., Zrnyi, M., & Chen, Y. M. (2015). Novel biocompatible polysaccharide-based self-healing hydrogel. *Advanced Functional Materials*, 25(9), 1352–1359.
- Wulle, F., Gorke, O., Schmidt, S., Nistler, M., Tovar, G. E., Riedel, O., & Southan, A. (2022). Multi-axis 3D printing of gelatin methacryloyl hydrogels on a non-planar surface obtained from magnetic resonance imaging. *Additive Manufacturing*, 50, Article 102566.
- Xing, Q., Yates, K., Vogt, C., Qian, Z., Frost, M. C., & Zhao, F. (2014). Increasing mechanical strength of gelatin hydrogels by divalent metal ion removal. *Scientific Reports*, 4(1), 1–10.
- Xu, Q., Ji, Y., Sun, Q., Fu, Y., Xu, Y., & Jin, L. J. N. (2019). Fabrication of Cellulose Nanocrystal/Chitosan Hydrogel for Controlled Drug Release., 9(2), 253.
- Yeo, Y. H., & Park, W. H. (2021). Dual-crosslinked, self-healing and thermo-responsive methylcellulose/chitosan oligomer copolymer hydrogels. *Carbohydrate Polymers*, 258, Article 117705.
- Zhang, Y. F., Zhang, N., Hingorani, H., Ding, N., Wang, D., Yuan, C., & Ge, Q. (2019). Fast-response, stiffness-tunable soft actuator by hybrid multimaterial 3D printing. *Advanced Functional Materials*, 29(15), 1806698.
- Zhang, Y. S., & Khademhosseini, A. (2017). Advances in engineering hydrogels. *Science*, 356(6337).
- Zhou, L., Ramezani, H., Sun, M., Xie, M., Nie, J., Lv, S., & He, Y. (2020). 3D printing of high-strength chitosan hydrogel scaffolds without any organic solvents. *Biomaterials Science*, 8(18), 5020–5028.
- Zhou, L. Y., Fu, J., & He, Y. (2020). A review of 3D printing technologies for soft polymer materials. *Advanced Functional Materials*, 30(28), 2000187.
- Zhu, W., Zhang, J., Wei, Z., Zhang, B., & Weng, X. (2023). Advances and Progress in self-healing hydrogel and its application in regenerative medicine. *Materials*, 16(3), 1215.